

# Hadamard Attention Recurrent Transformer: A Strong Baseline for Stereo Matching Transformer

Ziyang Chen<sup>✉</sup>, *Student Member, IEEE*, Yongjun Zhang<sup>\*✉</sup>, *Member, IEEE*, Wenting Li<sup>✉</sup>,  
Bingshu Wang<sup>✉</sup>, Yabo Wu<sup>✉</sup>, Yong Zhao<sup>✉</sup>, *Member, IEEE*, C. L. Philip Chen<sup>✉</sup>, *Life Fellow, IEEE*

**Abstract**—In light of the advancements in transformer technology, extant research posits the construction of stereo transformers as a potential solution to the binocular stereo matching challenge. However, constrained by the low-rank bottleneck and quadratic complexity of attention mechanisms, stereo transformers still fail to demonstrate sufficient nonlinear expressiveness within a reasonable inference time. The lack of focus on key homonymous points renders the representations of such methods vulnerable to challenging conditions, including reflections and weak textures. Furthermore, a slow computing speed is not conducive to the application. To overcome these difficulties, we present the Hadamard Attention Recurrent Stereo Transformer (HART) that incorporates the following components: 1) For faster inference, we present a Hadamard product paradigm for the attention mechanism, achieving linear computational complexity. 2) We designed a Dense Attention Kernel (DAK) to amplify the differences between relevant and irrelevant feature responses. This allows HART to focus on important details. DAK also converts zero elements to non-zero elements to mitigate the reduced expressiveness caused by the low-rank bottleneck. 3) To compensate for the spatial and channel interaction missing in the Hadamard product, we propose MKOI to capture both global and local information through the interleaving of large and small kernel convolutions. Experimental results demonstrate the effectiveness of our HART. In reflective area, HART ranked 1st on the KITTI 2012 benchmark among all published methods at the time of submission. Code is available at <https://github.com/ZYangChen/HART>.

**Index Terms**—Hadamard Attention, Efficient Transformer, Stereo Matching.

## I. INTRODUCTION

**S**TEREO matching represents a fundamental challenge in the field of computer vision, with a range of practical applications including autonomous driving, remote sensing, robotics and augmented reality [1]–[4]. The goal of stereo matching is to compute the pixel-by-pixel correspondences between two images, and to generate a disparity map that

Ziyang Chen, Yongjun Zhang, and Yabo Wu are with the College of Computer Science, the State Key Laboratory of Public Big Data, Guizhou University, Guiyang 550025, China (e-mail: ziyangchen2000@gmail.com, zyj6667@126.com, gs.wuyb22@gzu.edu.cn).

Wenting Li is with the School of Information Engineering, Guizhou University of Commerce, Guiyang 550021, China (e-mail: 201520274@gzcc.edu.cn).

Bingshu Wang is with the School of Software, Northwestern Polytechnical University, Xi'an, 710129, China (e-mail: wangbingshu@nwpu.edu.cn).

Yong Zhao is with the Key Laboratory of Integrated Microsystems, Shenzhen Graduate School, Peking University, Shenzhen 518055, China (e-mail: zhaoyong@pkusz.edu.cn).

C. L. Philip Chen is with the School of Computer Science and Engineering, South China University of Technology, Guangzhou 510641, China (e-mail: philip.chen@ieee.org).

\* Corresponding author: Yongjun Zhang.

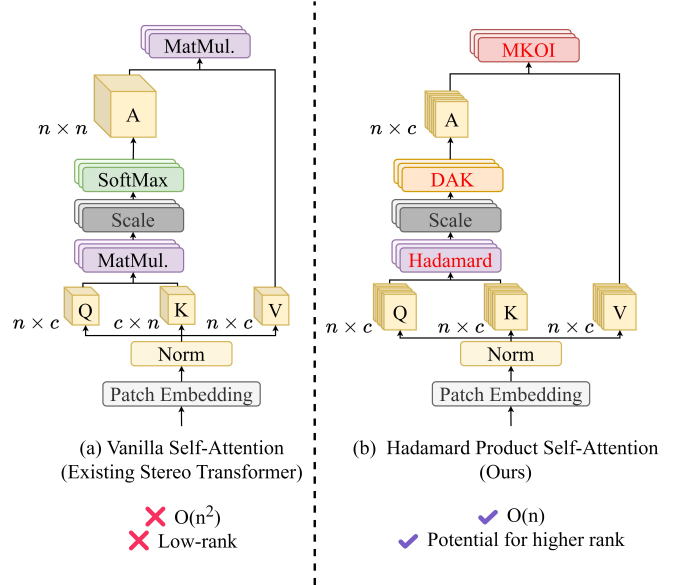


Fig. 1. **Motivation.** The ability to effectively and efficiently express in ill-posed regions, i.e. reflective area, is a crucial aspect of the stereo matching application. The low-rank bottleneck and the quadratic time complexity present significant challenges for stereo transformers in meeting the aforementioned needs. Our objective is to address these issues through the implementation of HART.

can be translated into depth using the settings of the stereo camera system [5]. In practical, it requires both high accuracy and speed. Consequently, the attainment of efficient stereo matching represents a crucial objective.

Since the development of deep learning, numerous stereo matching Convolutional Neural Networks (CNNs) have been presented. Recently, recurrent-based methods have shown promising performance on stereo matching benchmarks. RAFT-Stereo [6] uses a Recurrent All-pairs Field Transform (RAFT) [7] paradigm based on multi-level convolutional Gated Recurrent Units (convGRU). IGEV-Stereo [8] proposes the Combined Geometry Encoding Volume (CGEV) instead of the All-pairs Correlation (APC) Volume [6] in RAFT-Stereo. MoCha-Stereo [9] mining the recurrent feature in the feature channels and achieves state-of-the-art (SOTA) performance. However, the limited receptive field restricts the learning of long-range information. Recurrent-based methods face these challenges in matching local areas with unclear semantics, such as reflective regions and thin object areas.

The development of Vision Transformer (ViT) [10] has addressed the issue of acquiring long-range dependencies. STTR

[11] uses a transformer architecture, replacing cost volume construction with dense pixel matching from a sequence-to-sequence correspondence perspective. ELNet [12] combines stereo transformers with a multi-scale cost volume. However, existing stereo transformers still have certain limitations. As show in Fig. 1, stereo transformers are still constrained by the quadratic-level complexity of attention, limiting the speed of inference. They are challenging to meet the efficient computational requirements of scenarios such as autonomous driving. Moreover, vanilla self-attention (SA) also falls into a low-rank bottleneck [13]. This implies that stereo transformers have limited nonlinear expressive power, making them prone to being affected by ill-posed regions, such as reflections and weak textures, during the localization of homonymy points.

To alleviate the above problems, **Hadamard Attention Recurrent Stereo Transformer (HART)**, a new baseline for stereo transformer is proposed. Our primary contributions can be summarized as follows:

- 1) To achieve an efficient design for stereo transformers, we propose a strategy of computing attention using the Hadamard product. This enables attention computation to be controlled within linear time complexity.
- 2) To circumvent the low-rank bottleneck inherent in vanilla SA, we design a Dense Attention Kernel (DAK) function, instead of using the SoftMax activation. DAK allows the rank of attention to have the potential to increase further.
- 3) To realize spatial and channel interactions, Multi Kernel & Order Interaction (MKOI) module is presented to learn global and local features.
- 4) HART ranked **1st** on the KITTI 2012 reflective leaderboard and **TOP 10** among all published methods at the time of submission. Furthermore, the attention structure of HART is scalable. HART has the potential to become a new baseline for stereo transformers.

## II. RELATED WORK

### A. Recurrent-based Stereo CNNs

Learning-based methods [9], [14], [15] have grown rapidly in recent years. Among them, recurrent-based algorithms stand out for their performance in real-world scenarios. As a representative of recurrent-based techniques, RAFT-Stereo [6] validates the effectiveness of the RAFT iteration [7] and the APC pyramid structure. Subsequent improvements mainly focus on the computation of matching costs in the stereo matching field. CREStereo [16] designs Adaptive Group Correlation Layer (AGCL) to compute the correlation of each feature map at different cascade levels separately, refining the differences independently through multiple iterations. IGEV-Stereo [8] computes an additional set of Geometry Encoding Volumes (GEV) for correlation calculation. MoCha-Stereo [9] restores geometric details lost in the feature channels and calculates a correlation based on recurrent patterns within the channels. This process results in a new cost volume termed Motif Channel Correlation Volume (MCCV). The utilization of MCCV has helped recurrent-based stereo CNNs achieve SOTA performance on many datasets.

Despite the leading performance of such methods, recurrent-based schemes typically use convolutional operations with

relatively small receptive fields. They are not conducive to learning global information [10]. This makes recurrent-based CNNs challenging in areas where the semantic interpretation cannot be determined from local geometric information alone.

### B. Linear Transformers

In other tasks where transformers [17] are applied, numerous studies [18], [19] have attempted to achieve linear attention. The implementation of linear transformers typically decouples the SoftMax operation and altering the calculation order to first compute  $K^T \times V$ . Nevertheless, this form of attention matrix also suffers from the low-rank problem [13]. Each query matrix  $Q$  and key matrix  $K$  for every attention head jointly comprise only  $\frac{2nc}{d}$  parameters, where  $n = h \times w$  represents the spatial dimension,  $h$  and  $w$  denote the height and width of feature maps separately,  $c$  represents the channel dimension,  $d$  means the number of attention heads. Meanwhile, the attention matrix  $A = Q \times K$ , where the number of parameters is  $n^2$ , satisfies  $\frac{2nc}{d} \ll n^2$ . The low-rank bottleneck results in a decrease in expressiveness [20].

### C. Stereo Transformers

Benefiting from the global learning capability of ViT [10], stereo transformers [11], [12], [21] deliver excellent performance. STTR [11] constructs a transformer module with alternating self-attention and cross-attention to compute feature descriptors. CroCo-Stereo [21] stacks vanilla SA and MLP-designed encoder and decoder.

Though the design of the transformer allows for long-range matching, it is a computationally expensive model. SA has quadratic time complexity. As a result, existing stereo transformers generally require longer inference times. Currently, there are efforts to reduce the time complexity of stereo transformers. DLNR [22] borrows ideas from the attention in Restormer [23] and the recurrent update in RAFT-Stereo [6]. It deviates from the vanilla spatial feature matmul product and instead designs a channel feature matmul product. However, like other recurrent-based methods, DLNR lacks the spatial interactions of vanilla SA. In addition, although the number of channels  $c$ , is much smaller than  $h \times w$ ,  $c^2$  is still much larger than  $h \times w$  in DLNR. This means that the SA computation of DLNR still has a time complexity of  $O(c^2)$ .

In summary, stereo transformers still face two main challenges: 1) High computational cost of SA; 2) Inaccurate detail due to low-rank bottleneck.

## III. METHOD

### A. Overview

We designed HART, a strong stereo transformer baseline via Linear time Hadamard product. This approach speeds up inference. Moreover, we believe that improving the matching performance of Stereo Transformers hinges on: 1) overcoming the low-rank bottleneck of SA; 2) ensuring interaction between spatial and channel features.

To further meet the accuracy requirements mentioned above, HART incorporates a series of new components made by

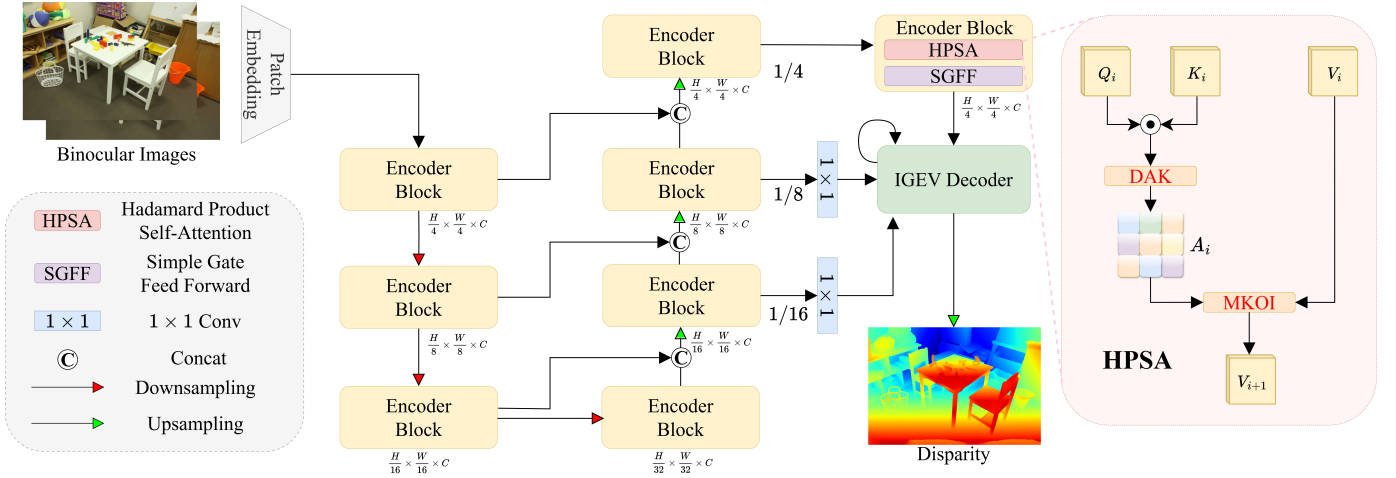


Fig. 2. The overall architecture of our HART. We construct multi-scale transformer blocks to encode features. The attention and forward propagation of the features are implemented by HPSA and SGFF respectively. We design the IGEV Decoder with reference to IGEV-Stereo. Based on the iterative updating paradigm and correlation volume, adaptations are made to the IGEV Decoder to suit our Stereo Transformer.

Hadamard product: 1) DAK is designed to learn attention matrix with all non-zero elements, ensuring that HART has the potential for continued rank increase. Additionally, DAK emphasizes important features by assigning them larger response values. 2) MKOI is proposed to supplement the spatial and cross-channel interaction capabilities lacking in the Hadamard product.

The details of the above designs are described in this section. To complete the HART workflow, we introduce techniques for iterative disparity updating and correlation computation as part of the decoder. The full architecture of HART is portrayed in Fig. 2. The Hadamard Product Self-Attention (HPSA) process is described in Sections III-B and III-C. The Simple Gate Feed Forward (SGFF) mechanism is detailed in Section III-D. HPSA and SGFF form the encoder of HART, while the decoder of HART is outlined in Section III-E. Inspired by STTR [11] and IGEV-Stereo [8], we supervised HART by the Equ. 1, where  $\gamma = 0.9$ ,  $N$  denotes the total number of iterations,  $d_0$  represents the initial disparity computed from correlation volume in our IGEV Decoder, and the loss for the initial disparity is calculated using smooth L1. L1 loss is used for subsequent iteration processes.

$$L = \text{Smooth}_{L1}(d_0 - d_{gt}) + \sum_{i=1}^N \gamma^{N-i} \|d_i - d_{gt}\|_1 \quad (1)$$

### B. Calculation of Attention Matrix

Although stereo transformers can achieve good results in long-range matching, this architecture is still not efficient enough. First, existing stereo transformers lack the non-linearity to convey complex scene detail. This is due to the low-rank bottleneck. Secondly, the quadratic complexity of the attention mechanism makes it difficult for transformers to achieve efficient performance. To achieve linear time complexity, HPSA is designed to be used here. We also implemented a series of designs to prevent HPSA from falling into the low-rank bottleneck.

1) *Hadamard Product between Query and Key*: Vanilla SA [10] in the Stereo Transformer [11], [12], [21] relies on matmul product to compute the attention matrix  $A$ . However, this computational approach exhibits a quadratic level of complexity.  $n = h \times w$  here,  $h$  denotes the height,  $w$  means width of the feature map.  $Q, K, V, A$  stand for query, key, value and attention matrix respectively. In existing Stereo Transformers, it holds that  $n \gg c$ . Consequently, the vanilla SA has a time complexity of  $O(n^2)$ . Despite the introduction of channel-wise SA [22], [23] for Stereo Transformer, the condition  $c^2 \gg n$  still prevails. To make attention more efficient, we have developed the HPSA as illustrated in Equ. 2.

$$A = \|Q\|_2 \odot \|K\|_2 \quad (2)$$

$$O(A) = O(Q_{c \times n} \odot K_{c \times n}) = O(c \cdot n) \triangleq O(n) \quad (3)$$

where  $\odot$  refers to the Hadamard product. The attention matrix  $A$  is computed solely through the Hadamard product of  $Q$  and  $K$ . According to Equ. 3, our attention calculation realises linear time complexity.

2) *Dense Attention Kernel (DAK)*: Attention matrix  $A$  comprises only  $n \times c$  parameters, and the  $Q$  and  $K$  matrices together consist of  $2nc$  parameters. This implies that, in theory, each parameter can be adequately represented. To achieve this, we aim for all parameters to maintain a non-zero state. Following this rationale, we have designed the Dense Attention Kernel (DAK), as depicted in Equ. 4. This non-zero state can alleviate the low-rank bottleneck [13], ensuring that pixel features can be expressed using a more diverse set of parameters.

$$\text{DAK}(A) = \begin{cases} A + 1, & A \geq 0 \\ e^A, & A < 0 \end{cases} \quad (4)$$

Different from ELU activation [24], our kernel function differs significantly in its underlying principles: 1) Our designed DAK aims to be utilized as an kernel function for attention. 2)

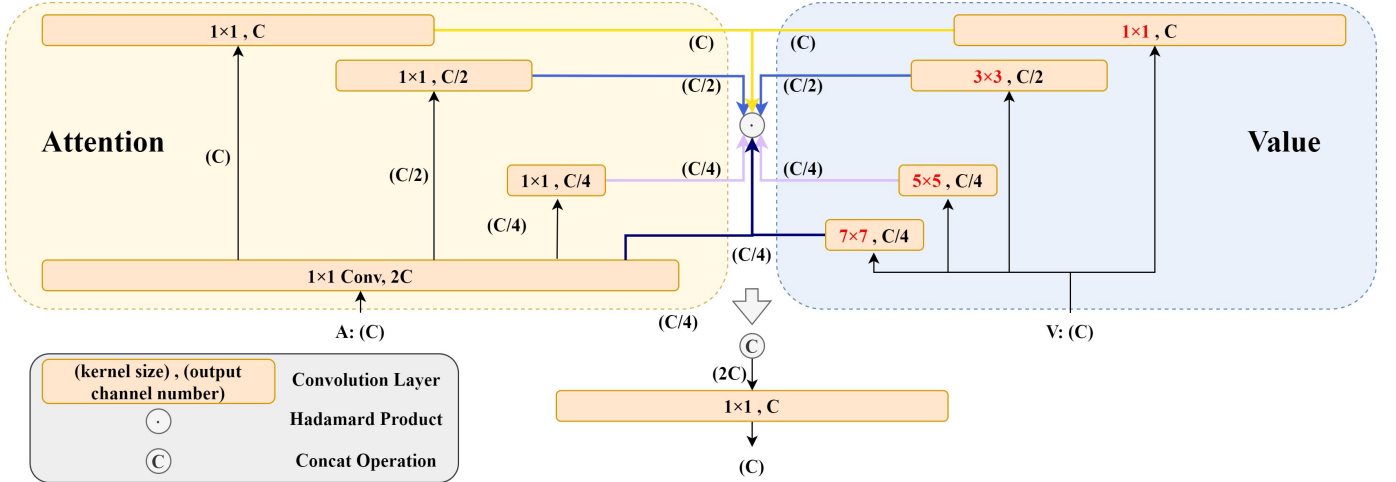


Fig. 3. Overview of Multi Kernel & Order Interaction (MKOI). The left box shows the splitting and convolution of the Attention matrix  $A$ , and the right box shows the splitting and convolution of the Value matrix  $V$ . It is worth noting that the letters in the brackets represent the number of channels. Lines of the same color represent the corresponding Hadamard product.

In comparison to the SoftMax utilized in vanilla SA and ELU used as activate function, our DAK always satisfied  $DAK(A) > 0$ . DAK suppresses the occurrence of silent neurons. Because zero elements in the matrix may become non-zero, there exists the theoretical possibility of an increase in the rank of the matrix. This implies that attention can have stronger non-linear expression capabilities. This design choice also involves assigning a smaller activation value to relatively less important dimensions. This serves as a weight in the description of the characteristics for the Value  $V$ .

We can ensure that each dimension is positively correlated with the weights here. Because the feature values of  $A$  at a given pixel are described by the channel features of that pixel. 3) In addition to amplifying the differences in attentional response scores, DAK shows more robust expressiveness than ELU. This is attributed to the fact that DAK can be decoupled into a process involving Equ. 5.

$$V_{i+1} = MKOI(DAK(A_i) \odot V_i) \triangleq MKOI(V_i + ELU(A_i) \odot V_i) \quad (5)$$

where  $V_i$  and  $V_{i+1}$  means Value before and after our attention processing, and  $ELU$  means ELU function. (See text in next section for content of MKOI.) Based on this formula, we can derive the gradient computation formula for the learning process of attention from shallow attention  $i$  to the deeper position  $I$  [25]. This process takes the form of Equ. 6.

$$\frac{\partial loss}{\partial V_i} = \frac{\partial loss}{\partial V_I} \cdot \frac{\partial V_I}{\partial V_i} \triangleq \frac{\partial loss}{\partial V_I} \cdot MKOI\left(1 + \frac{\partial}{\partial V_I} \sum_{j=i}^{I-1} (ELU(A_j) \cdot V_j)\right) \quad (6)$$

Furthermore, in contrast to the SoftMax function, which confines values to the  $[0, 1]$  interval, DAK extends the allocation of attention weights to the higher-dimensional interval  $(0, +\infty)$ . The derivative properties of DAK determine its ability to further widen the attentional gap, thereby redirecting the attention to more important features. The broader range of attentional

weighting contributes to a nuanced emphasis on key features. These ensure more diverse and focused feature representation, theoretically allowing for more precise matching.

### C. Multi Kernel & Order Interaction (MKOI)

Vanilla self-attention [10] satisfied  $SA(Q, K, V) = SoftMax\left(\frac{QK^T}{\sqrt{d_k}}\right)V$ . This process involves spatial and channel interactions. Vanilla Hadamard product cannot achieve this. To improve the spatial and channel interaction of HPSA, we propose the Multi Kernel & Order Interaction (MKOI) module as a complement to HPSA.

As shown in Fig. 3, MKOI is a Hadamard product paradigm concerning the Attention matrix  $A$  and the Value matrix  $V$ . To supplement the channel interaction capability, MKOI decouples features into four sets with channel numbers  $[c, c/2, c/4, c/4]$ , where  $c$  represents the original number of channels. The rough semantic distributions of the image are already implied by lower order features [26]. Therefore, we use large kernel convolutions to extract global semantic distributions. Compared to applying large kernel convolutions to all channels [27]–[29], this extraction mode is obviously cheaper. Higher-order features can focus on local features, so we use  $1 \times 1$  and  $3 \times 3$  convolutions to extract details. Through this paradigm, MKOI can capture both long-range and short-range information.

As a similar work,  $g^n Conv$  [30] is also a channel-wise operation. MKOI differs from  $g^n Conv$  mainly in two aspects. 1)  $g^n Conv$  only performs convolution within a specified kernel size, making it difficult to simultaneously focus on both global and local information. 2) The channel interaction of  $g^n Conv$  relies solely on the dot product operations between split features, resulting in a bottleneck in channel information interaction. MKOI achieves channel interaction between Attention features and Value features, enhancing attention to the

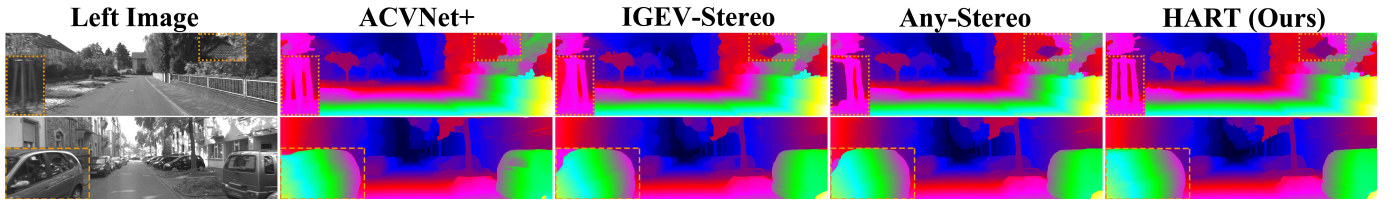


Fig. 4. Visualisation on the KITTI dataset [31]. We conducted comparisons with existing SOTA methods [8], [32], [33]. In the first image, HART accurately matches the details of the railing and correctly identifies the distant area between the tree leaves. In the second image, reflections on the car caused other methods to mis-match the outline of the car, while only HART achieved the correct match.

channels.

$$\begin{aligned}
 HPSA(Q, K, V) &= w_{1 \times 1}^{2c \rightarrow c} (\underbrace{[DAK(\|Q\|_2^{\frac{c}{2m}}) \odot \|K\|_2^{\frac{c}{2m}}]}_{\text{DAK}} \odot w_{s \times s}^{c \rightarrow \frac{c}{2m}}(V), \underbrace{[DAK(\|Q\|_2^{\frac{c}{4}}) \odot \|K\|_2^{\frac{c}{4}}]}_{\text{DAK}} \odot w_{7 \times 7}^{c \rightarrow \frac{c}{4}}(V)]_{m=\{0,1,2\}}} \\
 &\quad (7)
 \end{aligned}$$

$$V_{i+1} = HPSA(Q_i, K_i, V_i)$$

Overall, the HPSA combined with MKOI can be expressed by Equ. 7 and Fig. 1 (b). MKOI uses  $1 \times 1$  convolutions to compress and interact channels, producing  $V_{i+1}$  as input to the next transformer block.  $[\dots]$  means concat along the feature channel dimension here,  $s$  denotes the kernel size and  $s = 2m + 1$ .

#### D. Simple Gate Feed Forward (SGFF)

To complete the transformer architecture and further improve nonlinear expressiveness, we introduce a forward propagation architecture with reference to [23]. This process can be written as Equ.8.

$$\begin{aligned}
 Gate(V_{i+1}) &= GELU(w_{3 \times 3}^{c \rightarrow c}(V_{i+1}^{in})) \odot w_{3 \times 3}^{c \rightarrow c}(V_{i+1}^{in}) \\
 SGFF(V_i) &= w_{1 \times 1}^{c \rightarrow c}(Gate(w_{1 \times 1}^{c \rightarrow c}(V_{i+1}))) \quad (8)
 \end{aligned}$$

where  $GELU$  means GELU operation [34]. The overall computation process of our transformer block can be represented as Equ. 9.

$$\begin{aligned}
 Block_{att}(V^{init}) &= V^{init} + HPSA(Q, K, V) \\
 V_{i+1} &= Block_{att}(V_i) + SGFF(LN(Block_{att}(V_i))) \quad (9)
 \end{aligned}$$

where  $Block$  means the our transformer block in Fig. 2,  $LN$  denotes to Layer Normalization [35].  $Q$ ,  $K$ , and  $V$  here are three variables derived from the initial feature  $V^{init}$ . A  $1 \times 1$  convolutional layer is employed to produce features  $V^{3c}$  with a channel size of  $3c$ . These features are then evenly split into three parts along the channel dimension, representing  $Q$ ,  $K$ , and  $V$  respectively.

#### E. IGEV Decoder

The encoding structure of HART already demonstrates excellent capabilities, retaining long-term memory also aids in enhancing the disparity decoding abilities. We have therefore replaced the convGRU recurrent updating operator with LSTM-structured, inspired by [9], [22], [36], [37]. Outputs of this iterative update operation are added as increments to the previously calculated disparity values from the  $i$ -th iteration. For correlation volume, we follow IGEV-Stereo [8]

TABLE I  
DEFAULT HYPERPARAMETERS OF HART.

use mixed precision	True
batch size used during training	8
crop size	$320 \times 720$
max learning rate	0.0002
length of training schedule	200000
recurrent-number during training	22
Weight decay in optimizer	0.00001
recurrent-number during evaluation	32
number of levels in the correlation pyramid	2
width of the correlation pyramid	4
resolution of the disparity field ( $1/2^\circ K$ )	2
number of hidden recurrent levels	3
max disp of correlation encoding volume	192
color saturation	[0, 1.4]
random seed	666

to compute a group-wise correlation volume, and refine it with a regularization network  $\mathbb{R}$ .

$$\begin{aligned}
 \mathbb{C}_{GEV}(d, h, w, g) &= \mathbb{R} \left( \frac{1}{N_c/N_g} \langle f_{l,4}^g(h, w), f_{r,4}^g(h, w+d) \rangle, F(l) \right) \quad (10)
 \end{aligned}$$

where  $N_c$  is the number of channels,  $N_g$  means the group number ( $N_g = 8$  here),  $d$  denotes to the disparity level,  $\langle \dots, \dots \rangle$  is the inner product,  $F$  is a frozen network pretrained by [38],  $l$  is the left view image. The construction of 3D regularization network  $\mathbb{R}$  also follows IGEV-Stereo [8].

## IV. EXPERIMENT

### A. Implementation Details

The PyTorch framework is used to implement HART. The AdamW optimizer [56] is used during training. Tab. I collates the hyperparameters used by HART. The KITTI 2012 [57], KITTI 2015 [31], Scene Flow [58], and Middlebury [39] datasets were used to assess the performance of our model. HART is trained for 200,000 steps on the Scene Flow [58] dataset with a batch size of 8. The input photographs are cropped at random to  $320 \times 736$  pixels. We use data augmentation methods including spatial transformations and asymmetric chromatic augmentations. For training on the Middlebury dataset [39], we begin by fine-tuning the Scene Flow [58] pretrained model with a crop size of  $384 \times 512$  for 200,000 steps, using the mixed Tartan Air [59], CREStereo [16], Scene Flow [58], Falling Things [60], InStereo2k [61], CARLA [62], and Middlebury [39] datasets. We then use a batch size of 8 for an additional 100,000 steps to refine the model on the mixed CREStereo dataset [16], Falling Things

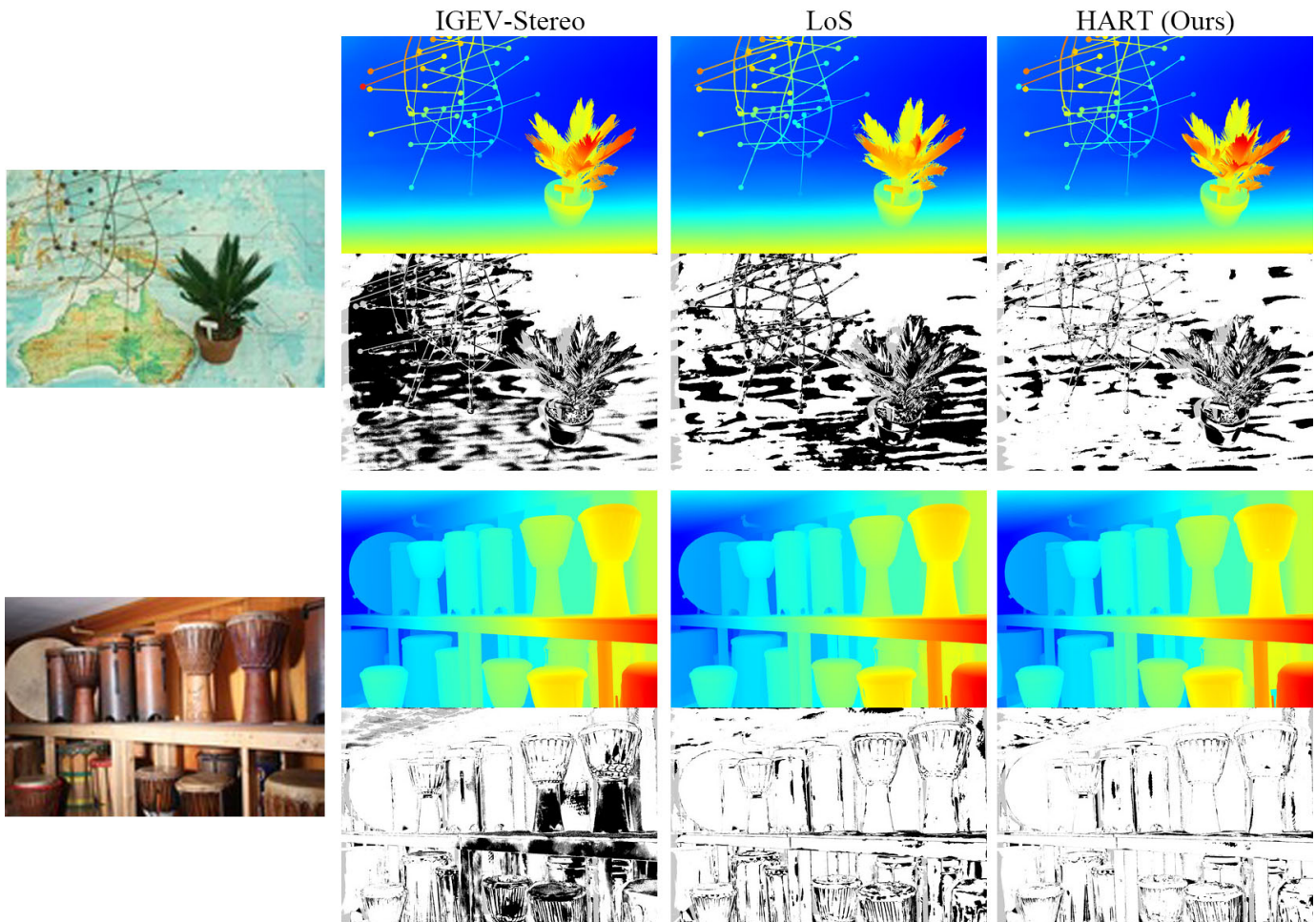


Fig. 5. Visualisation on the Middlebury dataset [39]. We conducted comparisons with existing SOTA methods [8], [40]. Disparity and error maps at 0.5 px threshold are included.

TABLE II  
 QUANTITATIVE EVALUATION ON SCENE FLOW TEST SET, THE 1-PIXEL ERROR RATE IS EMPLOYED (LOWER IS BETTER). THE BEST RESULTS ARE INDICATED IN BOLD AND THE SECOND-BEST RESULTS ARE UNDERSCORED. \* REFERS TO STEREO TRANSFORMER METHODS.

Method	Publish	EPE (px)↓	D1 (%)↓
GC-Net [41]	ICCV2017	1.84	15.6
PSMNet [14]	CVPR2018	1.09	12.1
GANet [42]	CVPR2019	0.78	8.7
GwcNet [15]	CVPR2019	0.76	8.0
AANet [43]	CVPR2020	0.87	9.3
RAFT-Stereo [6]	3DV2021	0.61	6.5
ACVNet+ [32]	CVPR2022	0.48	<b>5.0</b>
IGEV-Stereo [8]	CVPR2023	0.47	5.3
UPFNet [44]	TCSVT2023	0.71	6.7
DMCA-Net [45]	TCSVT2023	0.64	6.9
Selective-IGEV [46]	CVPR2024	<u>0.44</u>	<b>5.0</b>
STTR [11] *	ICCV2021	0.45	-
CroCo-Stereo [21] *	ICCV2023	-	5.3
DLNR [22] *	CVPR2023	0.48	5.4
GOAT [47] *	WACV2024	0.47	5.6
HART (Ours) *	Ours	<b>0.42</b>	<b>5.0</b>

[60], InStereo2k [61], CARLA [62], and Middlebury datasets [39]. For training on the KITTI 2012 [57] and KITTI 2015 [31] datasets, we fine-tune the Scene Flow pretrained model on the combined KITTI 2012 and KITTI 2015 datasets for 50,000 steps.

### B. Comparisons with State-of-the-art

We contrast the SOTA methods on Scene Flow [58], KITTI [31], [57], and Middlebury [39] datasets. HART performs admirably on all of the datasets mentioned above.

**Scene Flow.** As shown in Tab. II, HART achieves SOTA performance on the Scene Flow dataset. It achieves a 10.6% error reduction on the EPE metric compared to GOAT [47], the SOTA Stereo Transformer, and by 6.0% on the D1 metric compared to CroCo-Stereo [21].

**Reflective Area.** Due to the stronger capability in capturing long-range information, HART can integrate global features to make more accurate matches in ill-posed regions, such as reflective area. HART ranked **1st** on the KITTI 2012 reflective benchmark at the time of submission, as shown in Tab. III.

**KITTI.** To evaluate the performance of HART in real-world scenarios, we conducted experiments on KITTI benchmarks. Stereo transformers exhibit a significant disadvantage in terms

TABLE III

RESULTS ON THE KITTI 2012 REFLECTIVE LEADERBOARD. “NOC” MEANS PERCENTAGE OF ERRONEOUS PIXELS IN NON-OCCLUDED AREAS, “ALL” MEANS PERCENTAGE OF ERRONEOUS PIXELS IN TOTAL. **BOLD**: BEST PERFORMANCE, UNDERLINE: SECOND BEST.

Method	Publish	D1>2px (%)		D1>3px (%)		D1>4px (%)	
		Noc	All	Noc	All	Noc	All
DPCTF-S [48]	TIP2021	9.92	12.30	6.12	7.81	4.47	5.70
CREStereo [16]	CVPR2022	9.71	11.26	6.27	7.27	4.93	5.55
NLCA-Net V2 [49]	TNNLS2022	11.20	13.19	6.17	7.65	4.06	5.19
IGEV-Stereo [8]	CVPR2023	7.29	8.48	4.11	4.76	2.92	3.35
P3SNet+ [50]	TITS2023	23.60	26.32	15.85	18.50	11.66	14.13
UCFNet [51]	TPAMI2023	9.78	11.67	5.83	7.12	4.15	4.99
GANet+ADL [52]	CVPR2024	8.57	10.42	4.84	6.10	3.43	4.39
Selective-IGEV [46]	CVPR2024	6.73	7.84	3.79	4.38	2.66	3.05
LoS [40]	CVPR2024	<u>6.31</u>	7.84	<u>3.47</u>	4.45	<u>2.41</u>	<u>3.01</u>
MoCha-Stereo [9]	CVPR2024	6.97	8.10	3.83	4.50	2.62	3.80
RiskMin [53]	ICML2024	7.57	9.60	4.11	5.51	2.87	3.74
MoCha-V2 [37]	arXiv	6.54	<u>7.79</u>	3.65	4.50	2.58	3.19
HART	Ours	<b>6.18</b>	<b>7.38</b>	<b>3.14</b>	<b>3.92</b>	<b>1.99</b>	<b>2.49</b>

TABLE IV

RESULTS ON THE KITTI 2015 AND 2012. ERROR THRESHOLD IS 3 PX FOR 2015, AND 4 PX FOR 2012. FRONT-GROUND ERROR IS INDICATED BY “F.G.”, AND BACKGROUND ERROR BY “B.G.”. \* REFERS TO STEREO TRANSFORMER METHODS, WHICH ARE SUMMARIZED IN THE LOWER HALF OF THE TABLE. THE UPPER HALF OF THE TABLE DESCRIBES STEREO CNN METHODS. “TIME” DENOTES THE INFERENCE TIME ON SINGLE NVIDIA TESLA A100.

Method	Publish	2015 All		2015 Noc		2012		Time (s)
		F.G.	B.G.	F.G.	B.G.	Noc	All	
GwcNet [15]	CVPR2019	3.93	1.74	3.49	1.61	0.99	1.27	0.32
ACVNet+ [32]	CVPR2022	3.07	1.37	2.84	1.26	0.86	1.12	0.20
ADCPNet [54]	TCSVT2022	7.58	3.27	7.00	3.04	-	-	<b>0.01</b>
IGEV-Stereo [8]	CVPR2023	2.67	1.38	2.62	1.27	0.87	1.12	0.32
UPFNet [44]	TCSVT2023	2.85	<u>1.38</u>	2.70	<u>1.26</u>	-	-	0.25
DMCA-Net [45]	TCSVT2023	2.78	1.45	2.54	1.31	-	-	0.28
Any-Stereo [33]	AAAI2024	3.04	1.44	2.88	1.30	1.11	1.41	0.34
DKT-IGEV [55]	CVPR2024	3.05	1.46	3.01	1.36	-	-	<u>0.18</u>
LoS [40]	CVPR2024	2.81	1.42	2.66	1.29	<u>0.85</u>	1.06	0.19
Selective-IGEV [46]	CVPR2024	2.61	<b>1.33</b>	2.55	<b>1.22</b>	<b>0.84</b>	<u>1.07</u>	0.24
STTR [11] *	CVPR2021	3.61	1.70	-	-	-	-	0.88
CroCo-Stereo [21] *	ICCV2023	2.65	1.38	2.56	1.30	-	-	0.93
DLNR [22] *	CVPR2023	<u>2.59</u>	1.60	-	-	-	-	0.33
HART*	Ours	<b>2.49</b>	1.39	<b>2.50</b>	1.29	<b>0.84</b>	<b>1.05</b>	0.25

of time. This is primarily due to the quadratic time complexity of their SA. Although DLNR significantly outperforms other stereo transformers in terms of inference speed, it sacrifices spatial dimension interaction. Experimental results in Tab. IV and Fig. 4 confirm that, HART is still able to emphasise the matching of spatial details within a given inference time. While compared to SOTA methods, HART does exhibit some deficiencies in background matching. This attributed to our designs, which leads to focus more on foreground features.

**Middlebury.** HART is also able to achieve excellent performance in the Middlebury scenario. HART outperforms the SOTA method LoS [40] by **15.5%**, **15.1%**, **8.62%** and **11.3%** for the four metrics shown in Tab. V and Fig. 5.

### C. Zero-shot Generalization

Collecting stereo matching datasets poses significant challenges, and stereo matching in real-world scenes often requires training on a small dataset to obtain matching results in untrained real scenes. This places certain demands on the generalization performance of stereo matching models. Zero-shot generalization is a common experiment to test the

TABLE V  
RESULTS ON MIDDLEBURY. THE ERROR THRESHOLD ARE 0.5 PX AND 1 PX HERE.

Method	Publish	D1>0.5px		D1>1.0px	
		Noc	All	Noc	All
RAFT-Stereo [6]	3DV2021	27.7	33.0	9.37	15.1
IGEV-Stereo [8]	CVPR2023	32.4	36.6	9.41	13.8
DMCA-Net [45]	TCSVT2023	49.8	54.1	22.2	28.5
Any-Stereo [33]	AAAI2024	32.7	37.5	11.5	16.8
GANet+ADL [52]	CVPR2024	52.3	55.9	30.3	35.2
LoS [40]	CVPR2024	<u>30.3</u>	<u>35.1</u>	<u>9.05</u>	<u>14.2</u>
CSTR [63] *	ECCV2022	48.5	55.2	21.6	32.0
CroCo-Stereo [21] *	ICCV2023	40.6	44.4	16.9	21.6
GOAT [47] *	WACV2024	49.0	52.9	21.4	27.0
HART *	Ours	<b>25.6</b>	<b>29.8</b>	<b>8.27</b>	<b>12.6</b>

generalization performance of stereo matching. We follow the paradigm of training on Scene Flow and testing the model on real scenes from Middlebury, KITTI, and Driving Stereo [65] datasets to validate our generalization ability. The experimental results are presented in Tab. VI, Tab. VII and

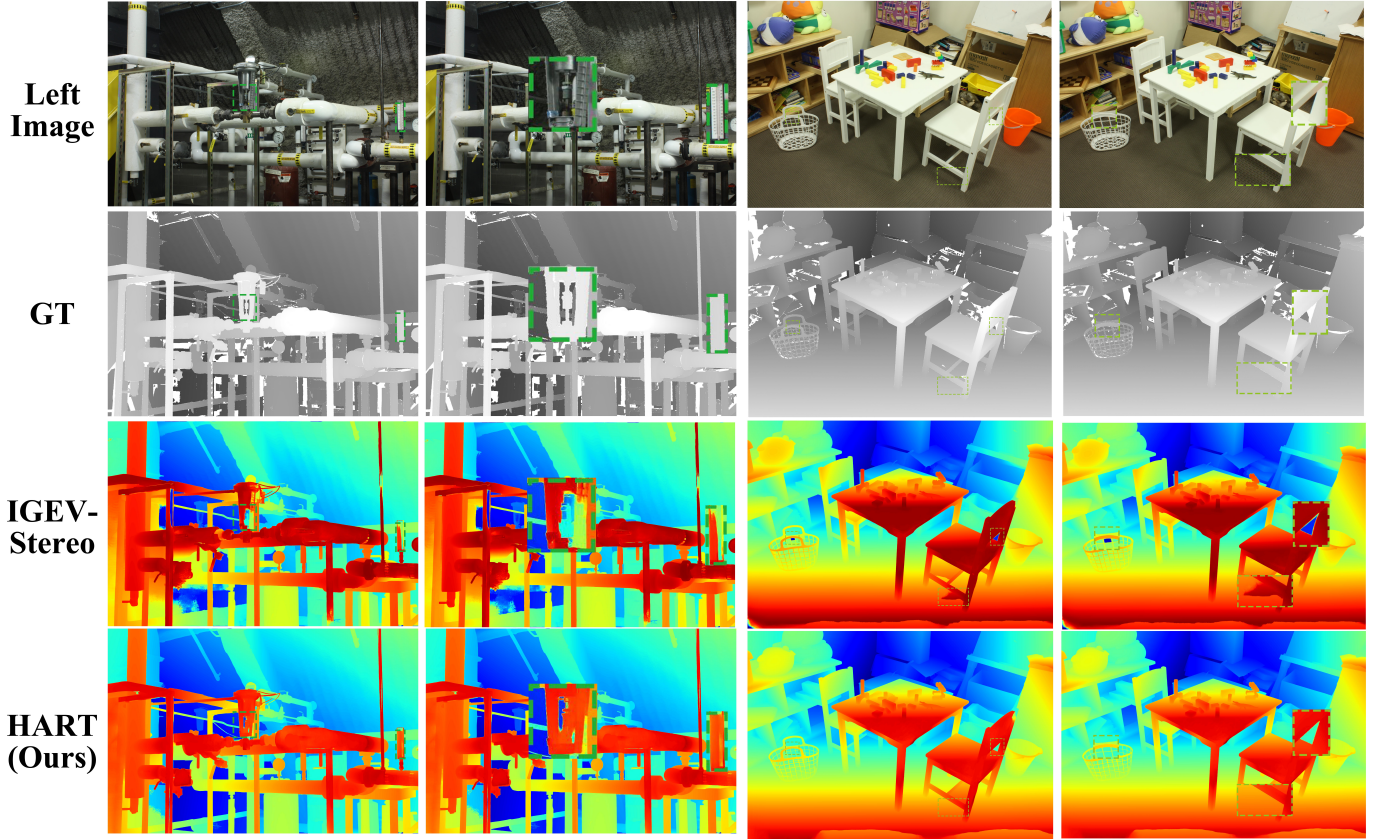


Fig. 6. Zero-shot evaluation without fine-tuning on Middlebury. All results visualised here are trained on Scene Flow. The odd-numbered columns show the original images, the even-numbered columns present zoomed-in details for better visualization.

TABLE VI

ZERO-SHOT EVALUATION ON MIDDLEBURY AND KITTI. EVERY MODEL UNDERGOES SCENE FLOW TRAINING WITHOUT FINE-TUNING. THE 2PX ERROR RATE IS EMPLOYED FOR MIDDLEBURY, AND 3PX ERROR RATE FOR KITTI.

Method	Publish	Middlebury↓			KITTI↓	
		F	H	Q	EPE	D1
PSMNet [14]	CVPR2018	39.5	15.8	9.8	1.8	-
CFNet [64]	CVPR2021	28.2	15.3	9.8	1.7	-
STTR [11]	ICCV2021	-	15.5	9.7	1.5	6.4
RAFT-Stereo [6]	3DV2021	23.4	12.6	7.3	1.3	6.4
ELFNet [12]	ICCV2023	-	10.0	7.9	1.6	<u>5.8</u>
DLNR [22]	CVPR2023	14.5	9.5	7.6	2.8	16.1
IGEV-Stereo [8]	CVPR2023	15.2	7.1	6.2	<u>1.2</u>	6.0
MoCha-Stereo [9]	CVPR2024	<u>12.4</u>	<u>6.2</u>	<u>4.9</u>	<u>1.2</u>	<u>5.8</u>
HART	Ours	<b>12.2</b>	<b>4.9</b>	<b>4.8</b>	<b>1.1</b>	<b>5.1</b>

TABLE VII

ZERO-SHOT EVALUATION ON THE DRIVING STEREO DATASET. THE METRIC USED IS THE END POINT ERROR (EPE) ON THE FULL-RESOLUTION (F) AND HALF-RESOLUTION (H) IMAGES.

Method	Publish	Sunny		Rainy		Cloudy		Foggy	
		F	H	F	H	F	H	F	H
DLNR [22]	CVPR2023	3.16	1.93	4.94	3.85	2.45	1.85	3.47	2.63
MoCha-Stereo [9]	CVPR2024	<u>1.92</u>	1.19	4.21	2.37	1.93	<b>0.99</b>	<u>2.00</u>	0.98
Selective-IGEV [46]	CVPR2024	2.18	<u>1.18</u>	5.46	<u>2.17</u>	2.15	<u>1.12</u>	2.32	1.10
HART	Ours	<b>1.74</b>	<b>1.02</b>	<b>2.97</b>	<b>1.40</b>	<b>1.70</b>	<b>0.99</b>	<b>1.74</b>	<b>0.94</b>

TABLE VIII

ABLATION STUDY. ERROR THRESHOLD IS 3 PX. “ID” MEANS IGEV DECODER, “HP” DENOTES TO THE HADAMARD PRODUCT BETWEEN QUERY AND KEY HERE. THE FOLLOWING METRICS REPRESENT THE RESULTS OBTAINED FROM TRAINING AND TESTING ON THE SCENE FLOW DATASET. “TIME” DENOTES THE INFERENCE TIME ON SINGLE NVIDIA TESLA A100.

No.	STTR Encoder	HPSA Encoder				ID	EPE (px)	D1 (%)	Time (s)
		HP	SoftMax	DAK	MKOI				
1	-	-	-	-	-	0.47	2.47	0.37	
2	✓	-	✓	-	✓	0.44	2.38	0.71	
3	-	✓	✓	-	✓	0.49	2.46	<b>0.28</b>	
4	-	✓	-	✓	✓	0.46	2.43	<b>0.28</b>	
5	-	✓	✓	-	✓	0.43	2.39	0.36	
6	-	✓	-	✓	✓	<b>0.42</b>	<b>2.32</b>	0.36	

Fig. 6. The quantitative comparison results demonstrate the excellent generalization performance of HART.

D. Ablations

To validate the effectiveness of our design, we conduct ablation studies by individually removing each module. All experiments are conducted on the Scene Flow [58] dataset, and all hyperparameters are kept consistent with [8]. The results of the ablation experiments are shown in Tab. VIII.

**Baseline No.1: Recurrent Stereo CNN.** Our No.1 baseline is IGEV-Stereo [8]. Experiment No.1 in Tab. VIII demonstrates the performance of this method. Our transformer decoder borrows its code related to iterative updating and correlation calculation.

**Baseline No.2: Recurrent Stereo Transformer.** Building upon STTR [11], we designed the STTR encoder with the IGEV Decoder, as introduced in Section III-E. The improved version of STTR (No. 2 Experiment) has achieved higher accuracy and faster inference time compared to the original STTR [11]. This improvement is attributed not only to the enhanced decoder, i.e., IGEV Decoder, but also to the adoption of techniques inspired by Restormer [23]. Specifically, the feed-forward propagation network of the encoder has been upgraded to the SGFF structure introduced in Section III-D. Through this combination, we obtained a Recurrent Stereo Transformer. The effectiveness of this Recurrent Stereo Transformer, which is based on the vanilla self-attention (SA), is showcased in Experiment No.2.

Despite achieving results surpassing the CNN paradigm using the vanilla attention mechanism [10], the square complexity of matrix multiplication significantly slowed down the inference time, rendering it unsuitable for efficient matching requirements in practical scenarios. To address this issue, we propose an improved version of transformer encoder called HPSA, and utilize a series of novel designs to ensure its performance.

**Hadamard Product between Query and Key.** Hadamard product (HP) is the foundation of our HPSA. By utilizing the Hadamard product for attention computation, HART achieves linear attention computation. The effectiveness of this calculation is demonstrated in Experiment No.3. Although combining HP with the vanilla SoftMax activation function significantly reduces inference time, this approach encounters two issues.

TABLE IX

ABLATION STUDY FOR ITERATIONS. THE METRIC HERE IS END POINT ERROR

	Number of Iterations					
	1	2	3	4	8	32
RAFT-Stereo [6]	2.08	1.13	0.87	0.75	0.58	0.53
IGEV-Stereo [8]	0.66	0.62	0.58	0.55	0.50	0.47
Selective-IGEV [46]	0.65	0.60	0.56	0.53	0.48	0.44
HART(Ours)	<b>0.60</b>	<b>0.55</b>	<b>0.51</b>	<b>0.48</b>	<b>0.45</b>	<b>0.42</b>

TABLE X

ZERO-SHOT PERFORMANCE OF HART-DLNR. THE BASELINE HERE IS DLNR. OUR PROPOSED HPSA IS USED TO REPLACE SELF-ATTENTION MECHANISM (CATE) OF DLNR. ALL MODELS ARE TRAINED ON SCENE FLOW, AND TESTED ON MIDDLEBURY AND KITTI. THE THRESHOLD IS 2PX FOR MIDDLEBURY, AND 3PX FOR KITTI. “TIME (S)” IS THE INFERENCE TIME REQUIRED FOR THE MODEL TO RUN ON THE KITTI DATASET USING THE NVIDIA A100.

No.	Attention Mechanism	Middlebury↓			KITTI↓		Time (s)↓
		EPE	DI	EPE	DI		
1	CATE [22]	14.5	2.8	16.1		0.33	
2	HPSA w/ SoftMax	18.9	2.2	6.7		0.20	
3	HPSA w/ DAK	14.8	1.7	6.2		<b>0.19</b>	
4	HPSA w/ SoftMax+MKOI	12.8	1.6	5.8		0.28	
5	HPSA w/ DAK+MKOI (full model of HART-DLNR)	<b>9.9</b>	<b>1.4</b>	<b>5.0</b>		0.27	

1) The limitation of the SoftMax activation function prevents HART from overcoming the low-rank bottleneck [13] problem. 2) The Hadamard product lacks spatial and channel interactions, making it challenging to achieve satisfactory performance solely through the use of the Hadamard Product.

**Dense Attention Kernel (DAK).** DAK is proposed to address the low-rank bottleneck issue caused by SoftMax. Assigning larger differential activation values to the attention matrix can also make the matching features more precise. Comparative experiments No.3 and No.4 demonstrate the effectiveness of DAK.

**Multi Kernel & Order Interaction (MKOI).** The HPSA without MKOI can be represented by Equ. 11.

$$HPSA(Q, K, V)_{w/o MKOI} = DAK(\|Q\|_2 \odot \|K\|_2) \odot V \quad (11)$$

It is difficult to achieve spatial and channel feature interaction with this method, resulting in information loss. We developed

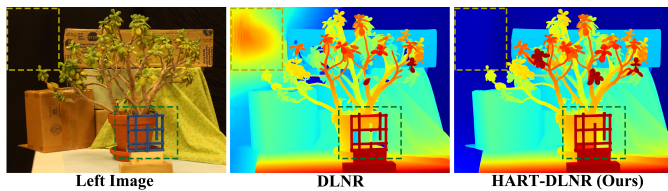


Fig. 7. Visualisation of the zero-shot performance comparison between [22] and our HART-DLNR. The results show that our HPSA can achieve better performance.

MKOI to overcome this shortcoming. Experiments No.5 and No.6 demonstrate the performance of MKOI.

**Number of Iterations** We adopted standard parameter settings and conducted our tests with 32 iterations. The architecture of HART enhances the effectiveness of the iterative strategy. HART achieves superior performance compared to other recurrent-based stereo methods across various iteration counts. To substantiate this claim, we compared HART against the SOTA Recurrent Stereo Transformer [22] and Recurrent Stereo CNN [8]. As shown in Tab. IX, experiments demonstrate that HART consistently outperforms other recurrent-based methods across various iteration counts.

#### E. Extension to existing Stereo Transformer

To further validate that our attention paradigm is a better way for stereo transformers, we applied HPSA from our HART to replace the Channel-Attention Transformer Extractor (CATE) from DLNR. DLNR is a representative Recurrent Stereo Transformer. Although CATE makes less inference time than other stereo transformers [12], [21], the trade-off is the loss of classical spatial interactions achieved by traditional ViTs. What is more, it still suffers from common issues inherent to stereo transformers. Firstly, CATE still exhibits quadratic time complexity, leaving room for improvement in inference time. Additionally, the parameter count for each attention head in CATE is still  $2nc/d$ , which remains significantly smaller than  $c^2$ . This implies that DLNR also faces the issue of low-rank bottleneck [13]. Compared to CATE in DLNR, HPSA offers the following advantages: 1) Further reduction in computational complexity; 2) Alleviating the low-rank bottleneck by using DAK; 3) Spatial dimension interaction has been achieved; 4) Improve the way channel dimensions interact. These benefits address the limitations of CATE and allow HPSA to replace CATE and achieve better outcomes. Experimental results shown in Fig. 7 and Tab. X demonstrate that HPSA designs improve the performance of DLNR and reduce the inference time.

## V. CONCLUSION

HART represents a novel approach to the transformer architecture. The objective is to surmount the intrinsic constraints of the square-level complexity and low-rank bottleneck, which have an adverse impact on the efficacy of stereo matching transformers. HART controls the time complexity within  $O(n)$  using the Hadamard product. DAK is established to focus on important features and to ensure the potential for rank

growth. MKOI is proposed to complement the spatial and channel interaction capabilities. These designs allow HART to achieve SOTA performance. Experimental results demonstrate the effectiveness of our HART. HART ranks **1st** on the KITTI 2012 reflective benchmark and **TOP 10** on the Middlebury benchmark among all published methods. While HART still has its limitation. HART is not able to achieve real-time at the moment. In the future, we plan to implement a faster solution and validate the effectiveness of HART in more frameworks.

## ACKNOWLEDGMENT

This work was supported in part by the Science and Technology Planning Project of Guizhou Province, Department of Science and Technology of Guizhou Province, China under Grant QianKeHe [2024] Key 001; and in part by the Science and Technology Planning Project of Guizhou Province, Department of Science and Technology of Guizhou Province, China under Grant [2023]159.

## REFERENCES

- [1] Z. Yuan, X. Song, L. Bai, Z. Wang, and W. Ouyang, "Temporal-channel transformer for 3d lidar-based video object detection for autonomous driving," *IEEE Trans. Circuit Syst. Video Technol.*, vol. 32, no. 4, pp. 2068–2078, 2021.
- [2] Z. Chen, W. Li, Z. Cui, and Y. Zhang, "Surface depth estimation from multi-view stereo satellite images with distribution contrast network," *IEEE J. Sel. Topics Appl. Earth Observ. Remote Sens.*, 2024.
- [3] X. Ye, J. Zhang, Y. Yuan, R. Xu, Z. Wang, and H. Li, "Underwater depth estimation via stereo adaptation networks," *IEEE Trans. Circuit Syst. Video Technol.*, vol. 33, no. 9, pp. 5089–5101, 2023.
- [4] G.-T. Michailidis, R. Pajarola, and I. Andreadis, "High performance stereo system for dense 3-d reconstruction," *IEEE Trans. Circuit Syst. Video Technol.*, vol. 24, no. 6, pp. 929–941, 2013.
- [5] Y. Zhan, Y. Gu, K. Huang, C. Zhang, and K. Hu, "Accurate image-guided stereo matching with efficient matching cost and disparity refinement," *IEEE Trans. Circuit Syst. Video Technol.*, vol. 26, no. 9, pp. 1632–1645, 2015.
- [6] L. Lipson, Z. Teed, and J. Deng, "Raft-stereo: Multilevel recurrent field transforms for stereo matching," in *Int. Conf. 3D Vis.* IEEE, 2021, pp. 218–227.
- [7] Z. Teed and J. Deng, "Raft: Recurrent all-pairs field transforms for optical flow," in *Eur. Conf. Comput. Vis.* Springer, 2020, pp. 402–419.
- [8] G. Xu, X. Wang, X. Ding, and X. Yang, "Iterative geometry encoding volume for stereo matching," in *IEEE Conf. Comput. Vis. Pattern Recog.*, 2023, pp. 21 919–21 928.
- [9] Z. Chen, W. Long, H. Yao, Y. Zhang, B. Wang, Y. Qin, and J. Wu, "Mocha-stereo: Motif channel attention network for stereo matching," in *IEEE Conf. Comput. Vis. Pattern Recog.*, 2024, pp. 27 768–27 777.
- [10] A. Dosovitskiy, L. Beyer, A. Kolesnikov, D. Weissenborn, X. Zhai, T. Unterthiner, M. Dehghani, M. Minderer, G. Heigold, S. Gelly *et al.*, "An image is worth 16x16 words: Transformers for image recognition at scale," *arXiv preprint arXiv:2010.11929*, 2020.
- [11] Z. Li, X. Liu, N. Drenkow, A. Ding, F. X. Creighton, R. H. Taylor, and M. Unberath, "Revisiting stereo depth estimation from a sequence-to-sequence perspective with transformers," in *Int. Conf. Comput. Vis.*, 2021, pp. 6197–6206.
- [12] J. Lou, W. Liu, Z. Chen, F. Liu, and J. Cheng, "Elfnet: Evidential local-global fusion for stereo matching," in *Int. Conf. Comput. Vis.*, 2023, pp. 17 784–17 793.
- [13] S. Bhojanapalli, C. Yun, A. S. Rawat, S. Reddi, and S. Kumar, "Low-rank bottleneck in multi-head attention models," in *Int. Conf. Mach. Learn.* PMLR, 2020, pp. 864–873.
- [14] J.-R. Chang and Y.-S. Chen, "Pyramid stereo matching network," in *IEEE Conf. Comput. Vis. Pattern Recog.*, 2018, pp. 5410–5418.
- [15] X. Guo, K. Yang, W. Yang, X. Wang, and H. Li, "Group-wise correlation stereo network," in *IEEE Conf. Comput. Vis. Pattern Recog.*, 2019, pp. 3273–3282.

- [16] J. Li, P. Wang, P. Xiong, T. Cai, Z. Yan, L. Yang, J. Liu, H. Fan, and S. Liu, "Practical stereo matching via cascaded recurrent network with adaptive correlation," in *IEEE Conf. Comput. Vis. Pattern Recog.*, 2022, pp. 16263–16272.
- [17] A. Vaswani, N. Shazeer, N. Parmar, J. Uszkoreit, L. Jones, A. N. Gomez, L. Kaiser, and I. Polosukhin, "Attention is all you need," *Adv. Neural Inform. Process. Syst.*, vol. 30, 2017.
- [18] S. Wang, B. Z. Li, M. Khabsa, H. Fang, and H. Ma, "Linformer: Self-attention with linear complexity," *arXiv preprint arXiv:2006.04768*, 2020.
- [19] Z. Shen, M. Zhang, H. Zhao, S. Yi, and H. Li, "Efficient attention: Attention with linear complexities," in *Proceedings of the IEEE/CVF winter conference on applications of computer vision*, 2021, pp. 3531–3539.
- [20] Y. Dong, J.-B. Cordonnier, and A. Loukas, "Attention is not all you need: Pure attention loses rank doubly exponentially with depth," in *Int. Conf. Mach. Learn.* PMLR, 2021, pp. 2793–2803.
- [21] P. Weinzaepfel, T. Lucas, V. Leroy, Y. Cabon, V. Arora, R. Brégier, G. Csurka, L. Antsfeld, B. Chidlovskii, and J. Revaud, "Croco v2: Improved cross-view completion pre-training for stereo matching and optical flow," in *Int. Conf. Comput. Vis.*, 2023, pp. 17969–17980.
- [22] H. Zhao, H. Zhou, Y. Zhang, J. Chen, Y. Yang, and Y. Zhao, "High-frequency stereo matching network," in *IEEE Conf. Comput. Vis. Pattern Recog.*, 2023, pp. 1327–1336.
- [23] S. W. Zamir, A. Arora, S. Khan, M. Hayat, F. S. Khan, and M.-H. Yang, "Restormer: Efficient transformer for high-resolution image restoration," in *IEEE Conf. Comput. Vis. Pattern Recog.*, 2022, pp. 5728–5739.
- [24] D.-A. Clevert, T. Unterthiner, and S. Hochreiter, "Fast and accurate deep network learning by exponential linear units (elus)," *arXiv preprint arXiv:1511.07289*, 2015.
- [25] K. He, X. Zhang, S. Ren, and J. Sun, "Deep residual learning for image recognition," in *IEEE Conf. Comput. Vis. Pattern Recog.*, 2016, pp. 770–778.
- [26] M. D. Zeiler and R. Fergus, "Visualizing and understanding convolutional networks," in *Eur. Conf. Comput. Vis.* Springer, 2014, pp. 818–833.
- [27] G. Huang, Z. Liu, L. Van Der Maaten, and K. Q. Weinberger, "Densely connected convolutional networks," in *IEEE Conf. Comput. Vis. Pattern Recog.*, 2017, pp. 4700–4708.
- [28] A. Krizhevsky, I. Sutskever, and G. E. Hinton, "Imagenet classification with deep convolutional neural networks," *Adv. Neural Inform. Process. Syst.*, vol. 25, 2012.
- [29] C. Peng, X. Zhang, G. Yu, G. Luo, and J. Sun, "Large kernel matters—improve semantic segmentation by global convolutional network," in *IEEE Conf. Comput. Vis. Pattern Recog.*, 2017, pp. 4353–4361.
- [30] Y. Rao, W. Zhao, Y. Tang, J. Zhou, S. N. Lim, and J. Lu, "Hornet: Efficient high-order spatial interactions with recursive gated convolutions," *Adv. Neural Inform. Process. Syst.*, vol. 35, pp. 10353–10366, 2022.
- [31] M. Menze and A. Geiger, "Object scene flow for autonomous vehicles," in *IEEE Conf. Comput. Vis. Pattern Recog.*, 2015, pp. 3061–3070.
- [32] G. Xu, Y. Wang, J. Cheng, J. Tang, and X. Yang, "Accurate and efficient stereo matching via attention concatenation volume," *IEEE Trans. Pattern Anal. Mach. Intell.*, 2023.
- [33] Z. Liang and C. Li, "Any-stereo: Arbitrary scale disparity estimation for iterative stereo matching," in *AAAI*, vol. 38, no. 4, 2024, pp. 3333–3341.
- [34] D. Hendrycks and K. Gimpel, "Gaussian error linear units (gelus)," *arXiv preprint arXiv:1606.08415*, 2016.
- [35] J. L. Ba, J. R. Kiros, and G. E. Hinton, "Layer normalization," *arXiv preprint arXiv:1607.06450*, 2016.
- [36] Z. Chen, Y. Zhao, J. He, Y. Lu, Z. Cui, W. Li, and Y. Zhang, "Feature distribution normalization network for multi-view stereo," *The Vis. Comput.*, pp. 1–13, 2024.
- [37] Z. Chen, Y. Zhang, W. Li, B. Wang, Y. Zhao, and C. Chen, "Motif channel opened in a white-box: Stereo matching via motif correlation graph," *arXiv preprint arXiv:2411.12426*, 2024.
- [38] M. Tan and Q. Le, "Efficientnet: Rethinking model scaling for convolutional neural networks," in *Int. Conf. Mach. Learn.* PMLR, 2019, pp. 6105–6114.
- [39] D. Scharstein, H. Hirschmüller, Y. Kitajima, G. Krathwohl, N. Nešić, X. Wang, and P. Westling, "High-resolution stereo datasets with subpixel-accurate ground truth," in *Pattern Recognit. German Conf.* Springer, 2014, pp. 31–42.
- [40] K. Li, L. Wang, Y. Zhang, K. Xue, S. Zhou, and Y. Guo, "Los: Local structure-guided stereo matching," in *IEEE Conf. Comput. Vis. Pattern Recog.*, 2024, pp. 19746–19756.
- [41] A. Kendall, H. Martirosyan, S. Dasgupta, P. Henry, R. Kennedy, A. Bachrach, and A. Bry, "End-to-end learning of geometry and context for deep stereo regression," in *Int. Conf. Comput. Vis.*, 2017, pp. 66–75.
- [42] F. Zhang, V. Prisacariu, R. Yang, and P. H. Torr, "Ga-net: Guided aggregation net for end-to-end stereo matching," in *IEEE Conf. Comput. Vis. Pattern Recog.*, 2019, pp. 185–194.
- [43] H. Xu and J. Zhang, "Aanet: Adaptive aggregation network for efficient stereo matching," in *IEEE Conf. Comput. Vis. Pattern Recog.*, 2020, pp. 1959–1968.
- [44] Q. Chen, B. Ge, and J. Quan, "Unambiguous pyramid cost volumes fusion for stereo matching," *IEEE Trans. Circuit Syst. Video Technol.*, 2023.
- [45] K. Zeng, H. Zhang, W. Wang, Y. Wang, and J. Mao, "Deep stereo network with mrf-based cost aggregation," *IEEE Trans. Circuit Syst. Video Technol.*, 2023.
- [46] X. Wang, G. Xu, H. Jia, and X. Yang, "Selective-stereo: Adaptive frequency information selection for stereo matching," in *IEEE Conf. Comput. Vis. Pattern Recog.*, 2024, pp. 19701–19710.
- [47] Z. Liu, Y. Li, and M. Okutomi, "Global occlusion-aware transformer for robust stereo matching," in *IEEE Winter Conf. Appl. Comput. Vis.*, 2024, pp. 3535–3544.
- [48] Y. Deng, J. Xiao, S. Z. Zhou, and J. Feng, "Detail preserving coarse-to-fine matching for stereo matching and optical flow," *IEEE Trans. Image Process.*, vol. 30, pp. 5835–5847, 2021.
- [49] Z. Rao, Y. Dai, Z. Shen, and R. He, "Rethinking training strategy in stereo matching," *IEEE Trans. Neural Netw. Learn. Syst.*, vol. 34, no. 10, pp. 7796–7809, 2022.
- [50] A. Emlek and M. Peker, "P3snet: Parallel pyramid pooling stereo network," *IEEE Trans. Intell. Transp. Syst.*, vol. 24, no. 10, pp. 10433–10444, 2023.
- [51] Z. Shen, X. Song, Y. Dai, D. Zhou, Z. Rao, and L. Zhang, "Digging into uncertainty-based pseudo-label for robust stereo matching," *IEEE Trans. Pattern Anal. Mach. Intell.*, 2023.
- [52] P. Xu, Z. Xiang, C. Qiao, J. Fu, and T. Pu, "Adaptive multi-modal cross-entropy loss for stereo matching," in *IEEE Conf. Comput. Vis. Pattern Recog.*, 2024, pp. 5135–5144.
- [53] C. Liu, S. Kumar, S. Gu, R. Timofte, Y. Yao, and L. Van Gool, "Stereo risk: A continuous modeling approach to stereo matching," *arXiv preprint arXiv:2407.03152*, 2024.
- [54] H. Dai, X. Zhang, Y. Zhao, H. Sun, and N. Zheng, "Adaptive disparity candidates prediction network for efficient real-time stereo matching," *IEEE Trans. Circuit Syst. Video Technol.*, vol. 32, no. 5, pp. 3099–3110, 2021.
- [55] J. Zhang, J. Li, L. Huang, X. Yu, L. Gu, J. Zheng, and X. Bai, "Robust synthetic-to-real transfer for stereo matching," in *IEEE Conf. Comput. Vis. Pattern Recog.*, 2024, pp. 20247–20257.
- [56] I. Loshchilov, "Decoupled weight decay regularization," *arXiv preprint arXiv:1711.05101*, 2017.
- [57] A. Geiger, P. Lenz, and R. Urtasun, "Are we ready for autonomous driving? the kitti vision benchmark suite," in *IEEE Conf. Comput. Vis. Pattern Recog.* IEEE, 2012, pp. 3354–3361.
- [58] N. Mayer, E. Ilg, P. Hausser, P. Fischer, D. Cremers, A. Dosovitskiy, and T. Brox, "A large dataset to train convolutional networks for disparity, optical flow, and scene flow estimation," in *IEEE Conf. Comput. Vis. Pattern Recog.*, 2016, pp. 4040–4048.
- [59] W. Wang, D. Zhu, X. Wang, Y. Hu, Y. Qiu, C. Wang, Y. Hu, A. Kapoor, and S. Scherer, "Tartanair: A dataset to push the limits of visual slam," in *Int. Conf. Intell. Robots Syst.* IEEE, 2020, pp. 4909–4916.
- [60] J. Tremblay, T. To, and S. Birchfield, "Falling things: A synthetic dataset for 3d object detection and pose estimation," in *IEEE Conf. Comput. Vis. Pattern Recog.*, 2018, pp. 2038–2041.
- [61] W. Bao, W. Wang, Y. Xu, Y. Guo, S. Hong, and X. Zhang, "Instereo2k: a large real dataset for stereo matching in indoor scenes," *Sci. China Inf. Sci.*, vol. 63, pp. 1–11, 2020.
- [62] G. Yang, J. Manela, M. Happold, and D. Ramanan, "Hierarchical deep stereo matching on high-resolution images," in *IEEE Conf. Comput. Vis. Pattern Recog.*, 2019, pp. 5515–5524.
- [63] W. Guo, Z. Li, Y. Yang, Z. Wang, R. H. Taylor, M. Unberath, A. Yuille, and Y. Li, "Context-enhanced stereo transformer," in *Eur. Conf. Comput. Vis.* Springer, 2022, pp. 263–279.
- [64] Z. Shen, Y. Dai, and Z. Rao, "Cfnet: Cascade and fused cost volume for robust stereo matching," in *IEEE Conf. Comput. Vis. Pattern Recog.*, 2021, pp. 13906–13915.
- [65] G. Yang, X. Song, C. Huang, Z. Deng, J. Shi, and B. Zhou, "Driving-stereo: A large-scale dataset for stereo matching in autonomous driving scenarios," in *IEEE Conf. Comput. Vis. Pattern Recog.*, 2019, pp. 899–908.



**Ziyang Chen** (Student Member, IEEE) is currently working toward the master's degree with the College of Computer Science and Technology, Guizhou University, Guiyang, China. His major is Computer Science and Technology. He is supervised by Dr. Yongjun Zhang.

He has published several papers in journals and conferences, including *IEEE Conference on Computer Vision and Pattern Recognition (CVPR)*, and *IEEE Journal of Selected Topics in Applied Earth Observations and Remote Sensing*. His research interests lie in stereo matching, remote sensing, and intelligent transportation.



**Yongjun Zhang** (Member, IEEE) received the M.Sc. and PhD degrees in software engineering from Guizhou University, Guiyang, China in 2010 and 2015 respectively. From 2012 to 2015, he is a joint training doctoral student of Peking University, Beijing, China, and Guizhou University, studying in the key laboratory of integrated microsystems of Peking University Shenzhen Graduate School, Shenzhen, China.

He is currently an associate professor with Guizhou University. His research interests include the intelligent image algorithms of computer vision, such as scene target detection, remote sensing, stereo matching and low-level vision.



**Wenting Li** received the B.Sc. degree in computer science and technology from Zhengzhou University of Aeronautics, Zhengzhou, China, in 2006, the M.Sc. degree in computer science from Guizhou University, Guiyang, China, in 2010, and the Ph.D. degree in computer technology and application from the Macau University of Science and Technology, Macau, China, in 2017.

She is a professor with the Guizhou University of Commerce, Guiyang, China, since 2018. Her research interests include intelligent transportation, computer vision, and data analysis.



**Bingshu Wang** received the B.S. degree in computer science and technology from Guizhou University, Guiyang, China, in 2013, the M.S. degree in electronic science and technology (integrated circuit system) from Peking University, Beijing, China, in 2016, and the Ph.D. degree in computer science from the University of Macau, Macau, in 2020. He is currently an Associate Professor with the School of Software, Northwestern Polytechnical University, Suzhou, China. His current research interests include computer vision, intelligent video analysis, and machine learning.

machine learning.



**Yabo Wu** received the B.S. degree from the College of Computer Science and Technology, Guizhou University, Guiyang, China, in 2022. He is currently a postgraduate in the College of Computer Science and Technology, Guizhou University, Guiyang, China. He is supervised by Prof. Yongjun Zhang. His research interests include computer vision and pattern recognition.



**Yong Zhao** (Member, IEEE) received the Ph.D. degree in automatic control and applications from Southeast University, Nanjing, China, 1991. He then joined Zhejiang University, Hangzhou, China, as an Assistant Researcher. In 1997, he went to Concordia University, Montreal, QC, Canada, as a Post-Doctoral Fellow.

He was a Senior Audio/Video Compression Engineer with Honeywell Corporation, Mississauga, ON, Canada, in May 2000. In 2004, he became an Associate Professor at the Peking University Shenzhen Graduate School, Shenzhen, China, where he is currently the Header of the lab Mobile Video Networking Technologies. He is working on computer vision, machine learning, video analytics, and video compression with a special focus on applications of these new theories and technologies to various industries. His team has developed many innovative products and projects that have been successful in the market.



**C. L. Philip Chen** (Life Fellow, IEEE) was a recipient of the 2016 Outstanding Electrical and Computer Engineers Award from his alma mater, Purdue University (in 1988), after he graduated from the University of Michigan at Ann Arbor, Ann Arbor, MI, USA in 1985.

He is currently the Chair Professor and Dean of the College of Computer Science and Engineering, South China University of Technology. He is a Fellow of IEEE, AAAS, IAPR, CAA, and HKIE; a member of Academia Europaea (AE), and a member of European Academy of Sciences and Arts (EASA). He received IEEE Norbert Wiener Award in 2018 for his contribution in systems and cybernetics, and machine learning, received two times best transactions paper award from *IEEE Transactions on Neural Networks and Learning Systems* for his papers in 2014 and 2018 and he is a highly cited researcher by Clarivate Analytics from 2018-2022. His current research interests include cybernetics, systems, and computational intelligence. He was the Editor-in-Chief of the *IEEE Transactions on Cybernetics*, the Editor-in-Chief of the *IEEE Transactions on Systems, Man, and Cybernetics: Systems*, President of *IEEE Systems, Man, and Cybernetics Society*.